

A Centralized Reinforcement Learning Framework for Adaptive Clustering with Low Control Overhead in IoT Networks

F. Fernando Jurado-Lasso, *Member, IEEE*, J. F. Jurado, and Xenofon Fafoutis, *Senior Member, IEEE*

Abstract—Wireless Sensor Networks (WSNs) play a pivotal role in enabling Internet of Things (IoT) devices with sensing and actuation capabilities. Operating in remote and resource-constrained environments, these IoT devices face challenges related to energy consumption, crucial for network longevity. Clustering protocols have emerged as an effective solution to alleviate energy burdens on IoT devices. This paper introduces Low-Energy Adaptive Clustering Hierarchy with Reinforcement Learning-based Controller (LEACH-RLC), a novel clustering protocol that employs a Mixed Integer Linear Programming (MILP) for strategic selection of cluster heads (CHs) and node-to-cluster assignments. Additionally, it integrates a Reinforcement Learning (RL) agent to minimize control overhead by learning optimal timings for generating new clusters. Addressing key research questions, LEACH-RLC seeks to balance control overhead reduction without compromising overall network performance. Through extensive simulations, this paper investigates the frequency and opportune moments for generating new clustering solutions. Results demonstrate the superior performance of LEACH-RLC over conventional LEACH and LEACH-C, showcasing enhanced network lifetime, reduced average energy consumption, and minimized control overhead. The proposed protocol contributes to advancing the efficiency and adaptability of WSNs, addressing critical challenges in IoT deployments.

Index Terms—Internet of Things (IoT), Clustering Protocols, Reinforcement Learning (RL), Control Overhead, Low-Energy Adaptive Clustering Hierarchy (LEACH)

I. INTRODUCTION

The Internet of Things (IoT) is a term that refers to the interconnection of devices, sensors, and actuators to the Internet [1]. The IoT concept is based on the idea of connecting any device to the Internet, and it is not limited to computers and smartphones. It has gained popularity in recent years due to the advances in wireless communication technologies, the miniaturization of electronic devices, and

the development of low-cost sensors. IoT devices are key components of the fourth industrial revolution, also known as Industry 4.0 [2].

Wireless Sensor Networks (WSNs) are the backbone of the IoT concept as they provide the required infrastructure to connect devices to the Internet [3]. WSNs are composed of a large number of small devices, called ‘nodes’, that are deployed in an area of interest. These devices are equipped with sensors and actuators that allow them to collect data from the environment and interact with it. The integration of WSNs in IoT creates a cost-efficient networking infrastructure that can be used in a wide range of applications [4].

WSNs are often deployed in remote areas where changing or recharging the nodes’ batteries is not feasible [5], [6]. Therefore, the energy consumption of the nodes is a critical factor that determines the lifetime of the network. The energy consumption of the nodes is highly affected by the routing, which determines the path that the data will follow from the source node to the destination node, and the clustering, which determines the set of nodes that will act as cluster heads [4]. Clustering is a technique that is used to reduce the energy consumption of the nodes by grouping them into clusters. It is a two-step process consisting of selecting the Cluster Heads (CHs) and assigning the nodes to the clusters. CHs are responsible for collecting and aggregating data from the nodes that belong to their cluster and forwarding it to the Base Station (BS). Therefore, the routing and clustering protocols have a significant impact on the energy consumption of the nodes.

Among the clustering protocols proposed in the literature, Low-Energy Adaptive Clustering Hierarchy (LEACH) [7] has gained popularity due to its simplicity and low overhead. LEACH is a self-organizing protocol that allows the nodes to form clusters without the need for a centralized controller. Nodes’ roles are rotated periodically to distribute the energy consumption among the nodes. The CHs are selected stochastically in each round, and the nodes that are not CHs are assigned to the cluster that is closest to them. Cluster members send their data to the CH, whereas the CH sends the aggregated data directly to the BS. CHs also assigns a Time Division Multiple Access (TDMA) schedule to the nodes in their cluster to avoid collisions. Since CHs communicate directly with the BS, their communication cost is higher than the cost of the cluster members as they need to transmit data over a longer distance. Therefore, the selection of the CHs has a significant impact on the energy consumption of the nodes.

Manuscript received February 1, 2024; revised xx, xx. This work was partly supported by DAIS. DAIS (<https://dais-project.eu/>) has received funding from the ECSEL Joint Undertaking (JU) under grant agreement No 101007273. The JU receives support from the European Union’s Horizon 2020 research and innovation programme and Sweden, Spain, Portugal, Belgium, Germany, Slovenia, Czech Republic, Netherlands, Denmark, Norway, and Turkey. The document reflects only the authors’ view, and the Commission is not responsible for any use that may be made of the information it contains. Danish participants are supported by Innovation Fund Denmark under grant agreement No. 0228-00004A.

F. Fernando Jurado-Lasso and Xenofon Fafoutis are with the Embedded Systems Engineering section, DTU Compute, Technical University of Denmark, 2800 Lyngby, Denmark (e-mail: ffjla@dtu.dk; xefa@dtu.dk).

J. F. Jurado is with the Department of Basic Science, Faculty of Engineering and Administration, Universidad Nacional de Colombia Sede Palmira, Palmira 763531, Colombia (e-mail: jfjurado@unal.edu.co).

The selection of the set of CHs is a challenging problem. It is necessary to balance the energy consumption among the nodes and ensure that the CHs are evenly distributed across the network. While LEACH requires zero overhead to select the CHs, it does not guarantee that the CHs are evenly distributed across the network. To address this issue, Low-Energy Adaptive Clustering Hierarchy with Centralized Controller (LEACH-C) [8] was proposed. LEACH-C is an extension of LEACH that uses a centralized controller to select the CHs. The centralized controller has a global view of the network and can find the optimal set of CHs that minimizes the energy consumption of the nodes. LEACH-C use the annealing algorithm whose objective is to find the optimal set of CHs, at each round, that minimizes the squared distance between the nodes and their CHs.

While LEACH-C has demonstrated superior performance in terms of energy efficiency compared to LEACH, it has some limitations. Firstly, it relies on a centralized controller with a global view of the network. This controller is responsible for selecting the CHs and assigning the nodes to the clusters. However, making the controller aware of the network topology requires a significant amount of control messages. Consequently, the controller must periodically distribute control messages to the nodes, resulting in increased control overhead. Secondly, LEACH-C exclusively focuses on minimizing the squared distance between nodes and their respective CH. Yet, the energy consumption of nodes is also influenced by the distance between the CHs and the BS. Thirdly, LEACH-C does not take into account the energy consumption of CHs when receiving data from their cluster members. Consequently, the energy consumption of the CHs is not balanced with that of the cluster members.

A. Contributions

In this paper, we propose a novel clustering protocol, called Low-Energy Adaptive Clustering Hierarchy with Reinforcement Learning-based Controller (LEACH-RLC) ¹, that addresses the limitations of LEACH-C. LEACH-RLC formulates a Mixed Integer Linear Programming (MILP) to select the CHs and assign the nodes to the clusters, to minimize the overall energy consumption of the network. The MILP accounts for the energy consumption of nodes when transmitting data to their CHs and the energy consumption of the CHs when transmitting data to the BS and receiving data from their cluster members. Additionally, LEACH-RLC features a RL agent aimed at minimizing control overhead by learning the optimal time to send control messages. The key contributions of this paper include:

- 1) Introduction of LEACH-RLC, a novel clustering protocol utilizing a MILP for selecting CHs and assigning nodes to clusters.
- 2) Proposal of a RL agent to minimize control overhead by learning the optimal timing for generating new clusters.
- 3) Comparative analysis of the performance of LEACH-RLC with that of LEACH and LEACH-C.

¹The source code of LEACH-RLC is available at <https://github.com/fdojurado/PyNetSim.git>

- 4) Systematic investigation and answers to three key research questions (**RQ1**: Can we effectively reduce control overhead without compromising network performance? **RQ2**: How frequently should the controller initiate the generation of a new clustering solution? **RQ3**: When is the opportune moment for the controller to trigger a new clustering solution?).

The remainder of this paper is organized as follows. Section II presents the related work. Section III describes the system model. Section IV presents the proposed work for clustering. Section V presents the proposed work for control overhead minimization. Section VI presents the results. Finally, Section VII concludes the paper.

II. RELATED WORK

Efficient data collection and transmission with minimal energy consumption are primary goals in sensor networks, especially critical in battery-powered nodes deployed in remote IoT locations. While direct transmission is simple, its energy inefficiency over long distances is a concern. Clustering protocols address this by grouping nodes, reducing energy consumption. Over the past two decades, extensive research has focused on designing and implementing clustering protocols for IoT.

One pioneering clustering protocol is LEACH [7]. Nodes autonomously decide to be a CH or cluster member based on a threshold and random number. Expected numbers of CHs are determined by network size and desired CH percentage p , with nodes expected to become CHs every $1/p$ round. To address LEACH's limitations, LEACH-C aims to find the optimal set of CHs, minimizing node energy consumption [8]. A plethora of clustering protocols have stemmed from LEACH and LEACH-C.

A. Distributed Clustering Protocols

Behera et al. enhanced LEACH by modifying the threshold function to improve energy efficiency [9]. Threshold calculation considers node initial energy, residual energy, and the optimal number of CHs. Higher residual energy nodes are more likely to become CHs, preventing early network death. *Fathy et al.* proposed an adaptive data reduction technique for minimizing communication costs in IoT [10], using fine-grained sensor readings to reconstruct data and employing a dual prediction model. *Batta et al.* introduced an energy optimization clustering technique considering the State of Health (SOH) of sensor nodes' batteries [4], utilizing SOH to determine CH sets less prone to battery degradation. *Chithaluru et al.* suggested an adaptive fuzzy-based, cluster-based routing protocol for IoT [11], employing a fuzzy logic controller for volunteer node selection. *Behera et al.* improved the Stable Election Protocol [12], incorporating unique threshold strategies and reducing control overhead. *Chen et al.* proposed a 2-hop clustering protocol, considering the distance and residual energy of nodes to select CHs [13].

Lee et al. presented an energy-harvesting-aware clustering protocol for mobile WSN [14], [15] using a two-tier fuzzy inference system. *Ahmad et al.* proposed LEACH-MEEC,

TABLE I
COMPARISON OF RECENT CLUSTERING PROTOCOLS IN IOT

Article	Year	Clustering Type	AI/ML	Control Overhead	Key Features
[16]	2018	Distributed	✗	✗	LEACH-MEEC for mobile scenarios
[9]	2019	Distributed	✗	✗	Modified LEACH threshold
[10]	2019	Distributed	✗	✗	Adaptive data reduction
[12]	2019	Distributed	✗	✓	Improved Stable Election Protocol
[18]	2019	Centralized	✗	✗	Reducing energy consumption in mobile WSN
[14], [15]	2020	Distributed	✗	✗	Energy-harvesting-aware clustering
[11]	2021	Distributed	✗	✗	Fuzzy-based, cluster-based routing
[22]	2021	Centralized	✗	✗	Multi-hop routing for WSN
[23]	2021	Centralized	✗	✗	Adaptive Voronoi diagram-based clustering
[4]	2022	Distributed	✗	✗	Energy optimization considering SOH
[17]	2022	Distributed	✗	✗	Multi-path LEACH for mobility
[19]	2022	Centralized	✗	✓	Randomly centralized clustering
[20]	2022	Centralized	✗	✗	Energy consumption model estimation
[21]	2022	Centralized	✗	✗	Hybrid PSO and K-means strategy
[13]	2022	Distributed	✗	✗	2-hop clustering protocol
LEACH-RLC	2024	Centralized	✓	✓	MILP for CH selection and assignment, and RL for control overhead minimization

optimizing energy consumption in mobile scenarios [16]. *Mohapatra et al.* suggested energy-efficient clustering protocols for mobile scenarios [17], extending LEACH to multi-path LEACH protocols.

B. Centralized Clustering Protocols

LEACH-C has been foundational for other centralized clustering protocols. *Zhang et al.* proposed a centralized clustering protocol for mobile WSN [18], aimed at reducing node energy consumption while maximizing Packet Delivery Ratio (PDR). *Chen et al.* proposed a randomly centralized clustering protocol to alleviate workload [19], enabling bidirectional heartbeat messages for event-driven, on-demand cluster creation. *Tebessia et al.* proposed an energy consumption model on a centralized controller to estimate node energy consumption [20]. *Gamal et al.* introduced a hybrid PSO and K-means clustering strategy [21], extending network lifetime and improving stability. *Jin et al.* presented a multi-hop routing protocol for WSN [22], implementing the minimum spanning forest algorithm for intra-cluster and inter-cluster routing tree construction. *Ma et al.* proposed an adaptive Voronoi diagram-based clustering protocol [23] and a CH selection algorithm based on the weighted sum of the distance to the CH and the residual energy of the nodes.

C. Comparison with Related Work

To provide a comprehensive overview of clustering protocols in IoT, Table I presents a comparative analysis of various approaches, highlighting key aspects such as clustering type, incorporation of AI/ML techniques, handling of control overhead, and distinctive features of each protocol.

The significance of our work, LEACH-RLC, is underscored by its unique combination of features that directly address the limitations observed in existing clustering protocols for IoT networks. While prior protocols, such as those presented in the literature, have struggled to incorporate both optimal CH selection and efficient control overhead management simultaneously, LEACH-RLC stands out as a pioneering solution.

The majority of existing protocols ([9], [10], [4], [11], [14], [15], [16], [17], [18], [20], [22], [23], [13]) have primarily focused on specific aspects, such as modified thresholds, energy optimization, or clustering strategies, but have fallen short in simultaneously optimizing both energy efficiency and control overhead.

In contrast, LEACH-RLC introduces a centralized clustering protocol that not only leverages MILP for optimal CH selection and node-cluster assignments but also integrates a reinforcement learning agent. This agent is specifically designed to minimize control overhead by learning the optimal timing for sending control messages. This dual approach addresses the critical gap observed in the literature, making LEACH-RLC a groundbreaking advancement in the field of IoT clustering protocols.

III. SYSTEM MODEL

In our IoT network, N nodes are randomly deployed within a $L \times L$ area. Each node is equipped with an initial energy supply of E_0 and is identified by a unique identifier, i , along with coordinates (x_i, y_i) .

The communication graph $G = (N, \mathcal{E})$ represents the network, where N is the set of nodes and \mathcal{E} is the set of edges. Nodes collect data from the environment and transmit it to their respective CHs. CHs aggregate the data from their cluster members and send the aggregated data to the Base Station (BS), which is directly connected to the centralized controller.

The controller, equipped with a global network view, makes decisions on the optimal timing for creating new clusters, selecting CHs, and assigning nodes to clusters. Additionally, the controller manages the distribution of Time Division Multiple Access (TDMA) schedules to nodes.

The key assumptions in our model are as follows:

- 1) Nodes are static and do not change their positions during network operation.
- 2) Nodes are aware of their locations.
- 3) Nodes can adjust their transmission power settings.

TABLE II
NOTATION

Symbol	Description
N	$N = \{n_1, n_2, \dots, n_{ N }\}$ is the set of nodes in the network
L	Length of the area
E_0	Initial energy supply of nodes
E_i	Energy level of node i
E_i^d	$E_i^d = E_i^{r-1} - E_i^r$ is the energy dissipated by node i , and r and $r-1$ denote the current and previous rounds, respectively
\bar{E}_d	$\bar{E}_d = \frac{1}{ N } \sum_{i \in N} E_i^d$ is the average energy dissipated by the nodes in the network
E_{net}	$E_{net} = \sum_{i \in N} E_i$ is the total energy of the network at round r
\bar{E}	$\bar{E} = \frac{E_{net}}{ N }$ is the average energy level of the network
\mathcal{D}	$\mathcal{D} = \{n \in N E_n > 0\}$, $\mathcal{D} \subseteq N$ is the set of nodes currently active or operational
H	$H = \{n \in N E_n \geq \bar{E}\}$, $H \subseteq N$ is the set of potential cluster heads
C_i	Cluster of node i
CH	$CH = \{CH_1, CH_2, \dots, CH_{ N }\}$, $CH \subset N$ is the set of cluster heads
CH_r	Number of rounds elapsed since the last cluster head selection
CA	Current cluster assignment
E_{elec}	Energy consumed by the transmitter/receiver circuitry per bit
E_{fs}	Energy parameter for the free space model
E_{amp}	Energy parameter for the multi-path fading model
d_0	Threshold distance determining the transition between the free space and multi-path fading models
d_{ij}	Distance between nodes i and j
B_i	Packet size of node i
B_c	Control packet size
k	Percentage of nodes that are allowed to become CHs
$E_{tx}^{(i,j)}$	Energy consumed by node i when transmitting a packet of size B_i to node j
E_{rx}^i	Energy consumed by node i when receiving a packet of size B_i
$E_{rx}^{ch_i}$	Energy consumed by CH i when receiving data from its cluster members
$E_{tx}^{ch_i}$	Energy consumed by CH i when transmitting data to the BS
E_{DA}	Energy consumed by data aggregation
$E_{rx}^{c_i}$	Energy consumed by node i when receiving a control packet of size B_c
α	$\alpha \in \mathbb{R}_0^+$ is a weighting factor for the energy consumed by nodes when transmitting to CHs.
β	$\beta \in \mathbb{R}_0^+$ is a weighting factor for the energy consumed by CHs when transmitting to the sink.
γ	$\gamma \in \mathbb{R}_0^+$ is a weighting factor for the energy consumed by CHs when receiving from their cluster members.

4) The BS and controller remain stationary and are not resource-constrained after deployment.

We consider these assumptions reasonable for typical IoT applications. For example, in a smart city application, the BS and controller could be deployed in a fixed location, such as a building or a pole. Nodes, situated in the streets, may be powered by solar energy and equipped with Global Positioning System (GPS) receivers to determine their locations. The notation used throughout the paper is summarized in Table II.

A. Energy Consumption Model

To estimate the energy consumption of nodes, we adopt the widely recognized energy consumption model for WSN nodes proposed in [7]. This model integrates both the free space and multi-path fading models, selecting the appropriate model based on the distance between the transmitter and the receiver.

The threshold distance (d_0) determining the transition between the free space and multi-path fading models is calculated as follows:

$$d_0 = \sqrt{\frac{E_{fs}}{E_{amp}}} \quad (1)$$

where E_{fs} represents the energy parameter for the free space model, and E_{amp} is the energy parameter for the multi-path fading model.

The energy consumed by a node i when transmitting a packet of size B_i to a node j is given by:

$$E_{tx}^{(i,j)} = \begin{cases} E_{elec} \times B_i + E_{fs} \times B_i \times d_{ij}^2 & \text{if } d_{ij} \leq d_0 \\ E_{elec} \times B_i + E_{amp} \times B_i \times d_{ij}^4 & \text{otherwise} \end{cases} \quad (2)$$

where E_{elec} is the energy consumed by the transmitter or receiver circuitry per bit, and d_{ij} is the distance between nodes i and j .

The energy consumed when receiving a packet of size B_i is calculated as:

$$E_{rx}^i = E_{elec} \times B_i \quad (3)$$

CHs incur additional energy consumption due to the overhead of receiving and transmitting data within their clusters. Specifically, the energy consumed by a CH i when receiving data from its cluster members is given by:

$$E_{rx}^{ch_i} = E_{elec} \times \sum_{j \in C_i} B_j \quad (4)$$

where C_i denotes the set of nodes in the cluster of CH i .

Moreover, CHs consume energy when transmitting data to the BS. This energy consumption is expressed as:

$$E_{tx}^{ch_i} = (E_{elec} + E_{DA}) \times B_i + E_{tx} \quad (5)$$

where E_{DA} represents the energy consumed by data aggregation. The network incurs additional energy consumption due to the overhead of transmitting control packets, such as CH advertisements and CH selection messages. The energy consumed by a node i when receiving a control packet of size B_c is given by:

$$E_{rx}^{c_i} = E_{elec} \times B_c \quad (6)$$

IV. PROPOSED SOLUTION FOR CLUSTERING

In this section, we present the proposed solution for clustering. To address the challenges of CH selection and node assignment, we formulate a Mixed Integer Linear Programming (MILP) problem. We introduce the decision variables to formulate the MILP problem.

Variables	Description
$x_j, j \in H$	Binary variable indicating whether node j is selected as a CH.
$y_{ij}, i \in N, j \in H$	Binary variable indicating whether node i is assigned to CH j .

The resulting MILP problem is formulated as follows:

$$\min \alpha \sum_{i \in N} \sum_{j \in H} E_{tx}^{(i,j)} y_{ij} + \beta \sum_{j \in H} E_{tx}^{ch_j} x_j + \gamma \sum_{j \in H} \sum_{i \in N} E_{rx}^i y_{ij} \quad (7a)$$

$$\sum_{j \in H} y_{ij} = 1, \text{ for each } i \in N \quad (7b)$$

$$\sum_{j \in H} x_j = k \quad (7c)$$

$$y_{ij} \leq x_j, \text{ for each } i \in N, j \in H \quad (7d)$$

The objective function (7a) is designed to minimize the energy expended by non-CHs while transmitting to their respective CHs, the energy consumed by CHs during transmission to the sink, and the energy consumed by CHs during reception from their cluster members. The weighting factors α , β , and γ provide a mechanism for the MILP problem to prioritize different aspects of energy consumption.

The parameter α scales the energy spent by non-CHs during transmission to CHs, while β adjusts the energy used by CHs when transmitting to the sink. Meanwhile, γ influences the energy consumed by CHs during the reception from their cluster members. These weighting factors enable fine-tuning of the optimization process according to specific energy consumption priorities.

The constraints (7b), (7c), and (7d) contribute to the coherence and effectiveness of the clustering strategy. The first ensures that each node is assigned to exactly one CH, the second controls the selection of the desired number of CHs, and the third maintains consistency between x_j and y_{ij} , ensuring that if node j is not selected as a CH, then node i cannot be assigned to CH j .

The MILP problem not only minimizes overall energy consumption but also ensures a balanced workload distribution among the CHs. This comprehensive approach results in an energy-efficient and effective clustering strategy for IoT networks.

The majority of parameters in the MILP problem are static and derivable from the network model, including $E_{tx}^{(i,j)}$ and E_{rx} . Dynamic parameters, such as $H = \{n \in N | E_n \geq \bar{E}\}$, $H \subseteq N$, representing the set of potential CHs, are updated during each round of the clustering process. The only unknown parameters are the weighting factors α , β , and γ , whose values significantly influence the MILP problem's performance. Next, we explore an approach to determine these crucial parameter values.

A. Parameter Selection

The weighting factors α , β , and γ are crucial to the performance of the MILP problem. These parameters influence the optimization process and determine the clustering strategy's effectiveness. The values of these parameters are not known *a priori* and must be determined before the clustering process begins. Here, we present an approach to determine the values of these parameters.

To determine the values for the weighting factors, we systematically evaluate the performance of the MILP problem

for different values of α , β , and γ . We utilized the MILP problem to generate clustering solutions for a total of 600 combinations of (α , β , and γ), with each parameter ranging from 0 to 100. The evaluation of clustering solutions was based on the First Node Death (FND) metric, representing the number of rounds until the first node exhausts its energy. Figure 1 presents a heatmap illustrating the FND metric for diverse values of α , β , and γ .

1) *Heatmap of the FND metric*: The heatmap distinctly reveals the sensitivity of the FND metric to variations in α , β , and γ . Noteworthy observations include the following:

- Fig. 1a and Fig. 1c, the FND metric attains its peak when $\beta < 30$.
- Fig. 1a and Fig. 1b showcase that the FND metric is highest when $\alpha > 20$.
- Fig. 1b and Fig. 1c highlight that the FND metric achieves its maximum when $\gamma > 30$.

2) *Optimal Parameter Values*: These observations underscore the sensitivity of the FND metric to the specific values of α , β , and γ . The overall best performance is attained when employing the following parameter values: $\alpha = 54.83$, $\beta = 14.54$, and $\gamma = 35.31$. Importantly, these values are tailored to the network scenario discussed in Section VI.

These findings provide crucial insights for selecting optimal weighting factor values, ensuring enhanced energy efficiency and network longevity in the context of the proposed MILP-based clustering strategy.

V. PROPOSED SOLUTION FOR OVERHEAD REDUCTION

In this section, we introduce our innovative solution crafted to mitigate control overhead in the network, paving the way for improved network performance. We aim to address the following research questions:

- **RQ1**: Can we effectively reduce control overhead without compromising network performance?
- **RQ2**: How frequently should the controller initiate the generation of a new clustering solution?
- **RQ3**: When is the opportune moment for the controller to trigger a new clustering solution?

A. Proposed solution overview

In our quest to diminish control overhead, we propose the integration of a RL agent. This agent is designed to learn and discern the optimal timing for generating a new clustering solution, thereby streamlining the control process. Through the use of reinforcement learning, our solution seeks to strike a harmonious balance between minimizing control overhead and enhancing overall network efficiency. Readers interested in a comprehensive overview of reinforcement learning and its networking applications are referred to [24]–[27].

We cast the challenge of minimizing control overhead as a Markov Decision Process (MDP). The MDP is characterized by a tuple $\langle \mathcal{S}, \mathcal{A}, \mathcal{R} \rangle$, where \mathcal{S} denotes the set of states, \mathcal{A} signifies the set of actions, and \mathcal{R} encapsulates the reward function [28].

The state s_t at time t is comprehensively described by the tuple $\langle E_{net_t}, E_{n_t} \forall n \in N, CH_t, CH_{\tau_t}, CA_t, a_{t-1} \rangle$. Here, t

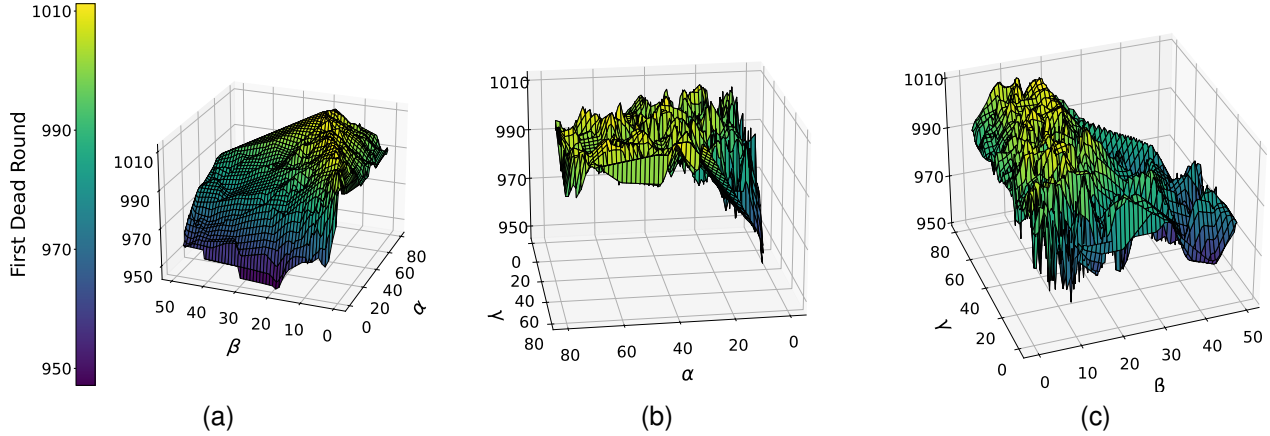


Fig. 1. Heatmap of the FND metric for different values of α , β , and γ .

also denotes the current round. In this representation, $E_{net_t} = \sum_{n \in N} E_n$ is the network's residual energy at time t , $E_{n_t} \forall n \in N$ captures the residual energy of individual nodes at time t , CH_t denotes the set of cluster heads, CH_{τ_t} indicates the number of rounds elapsed since the last cluster head selection, CA_t depicts the current cluster assignment, and $a_{t-1} \in \mathcal{A}$ denotes the action taken at time $t-1$.

Now, delving into the action space \mathcal{A} , the agent has the flexibility to choose from the following actions: *generate a new clustering solution* and *maintain the current clustering solution*. This action space is denoted as $\mathcal{A} = \{a_1, a_2\}$, where a_1 represents the action generating a new clustering solution, and a_2 corresponds to the action maintaining the current clustering solution.

The immediate reward function $\mathcal{R}(s, a)$ for the agent in the proposed MDP is designed to encourage behaviors that enhance the network's performance. At each time step, the agent is rewarded with 1 point if no nodes experience depletion in their energy, promoting the longevity of the network without node losses. Additionally, the agent receives a small reward of 0.1 when it chooses to generate a new clustering solution (a_1). This encourages the agent to explore new cluster configurations, facilitating adaptability to changing network conditions. Lastly, a higher reward of 2 is granted when the episode concludes, marking the end of a round. The episode concludes when the first node experiences energy depletion, reflecting the critical nature of node failures. This substantial reward is intended to signify the conclusion of the learning episode, capturing the significance of sustaining the network without premature node losses. Mathematically, the reward function is defined as follows:

$$\mathcal{R}(s_t, a_t) = \begin{cases} 1 & \text{if } a_t = a_2 \text{ and } E_{n_t} > 0 \text{ for all } n \in N \\ 1.1 & \text{if } a_t = a_1 \text{ and } E_{n_t} > 0 \text{ for all } n \in N \\ 2 & \text{if } E_{n_t} \leq 0 \text{ for some } n \in N \end{cases} \quad (8)$$

The proposed solution leverages the MILP described in Section IV to generate a clustering solution. However, the computational complexity of the MILP, even though invoked only when the agent opts to generate a new clustering solution, poses a potential bottleneck due to high training epochs. On

a 2.3 GHz 8-Core Intel Core i9 processor with 16 GB of RAM, the MILP requires approximately 0.91 ± 0.4 seconds to generate a new clustering solution. In contrast, the RL agent, introduced later, achieves the same task in just 0.0069 ± 0.0004 seconds. Recognizing the computational disparity, we address this challenge through a novel approach outlined in the subsequent section.

B. Neural network-based clustering solution prediction

To alleviate the computational complexity of the MILP, we advocate for the adoption of a neural network to predict the clustering solution. This innovative approach aims to streamline the computational demands associated with clustering while maintaining accuracy. The neural network is trained using the clustering solutions generated by the MILP as the ground truth. However, we adopt a nuanced strategy by breaking down the clustering solution into two distinct components: the set of CHs and the set of cluster members. The neural network is then trained to these two components separately. This architecture enhances prediction accuracy, especially considering the key role of the cluster heads' feature in determining the cluster members.

The neural network architecture for the cluster heads is designed to take as input the α , β and γ parameters, E_{net} , $E_n \forall n \in N$, F , \hat{E}_{tx}^{ch} , \hat{E}_{rx}^{ch} , and \widehat{CH} . Where $F = [F_1, F_2, \dots, F_{|N|}]$ is a binary vector indicating whether a node n is a potential cluster head ($F_n = 1$) or not. Node n is a potential cluster head $F_n = 1 \iff E_n \geq \bar{E}$, where \bar{E} is the average energy level of the network. $\hat{E}_{tx}^{ch} = [\hat{E}_{tx_1}^{ch}, \hat{E}_{tx_2}^{ch}, \dots, \hat{E}_{tx_{|N|}}^{ch}]$ is a vector containing the expected energy consumption of potential cluster heads when transmitting data to the BS. Here, $\hat{E}_{tx_n}^{ch} = E_{tx_n}^{ch}$ if $F_n = 1$, and $\hat{E}_{tx_n}^{ch} = 0$ otherwise. The vector $\hat{E}_{rx}^{ch} = [\hat{E}_{rx_1}^{ch}, \hat{E}_{rx_2}^{ch}, \dots, \hat{E}_{rx_{|N|}}^{ch}]$ is a representation of the expected energy consumption of potential cluster heads when receiving data from cluster members. For each potential cluster head n , $\hat{E}_{rx_n}^{ch}$ equals $E_{rx_n}^{ch}$ if $F_n = 1$, and is zero otherwise. $\widehat{CH} = k \times |\mathcal{D}|$ is the expected number of cluster heads, where $\mathcal{D} = \{n \in N | E_n > 0\}$, $\mathcal{D} \subseteq N$ denotes the set of nodes that are currently active or operational,

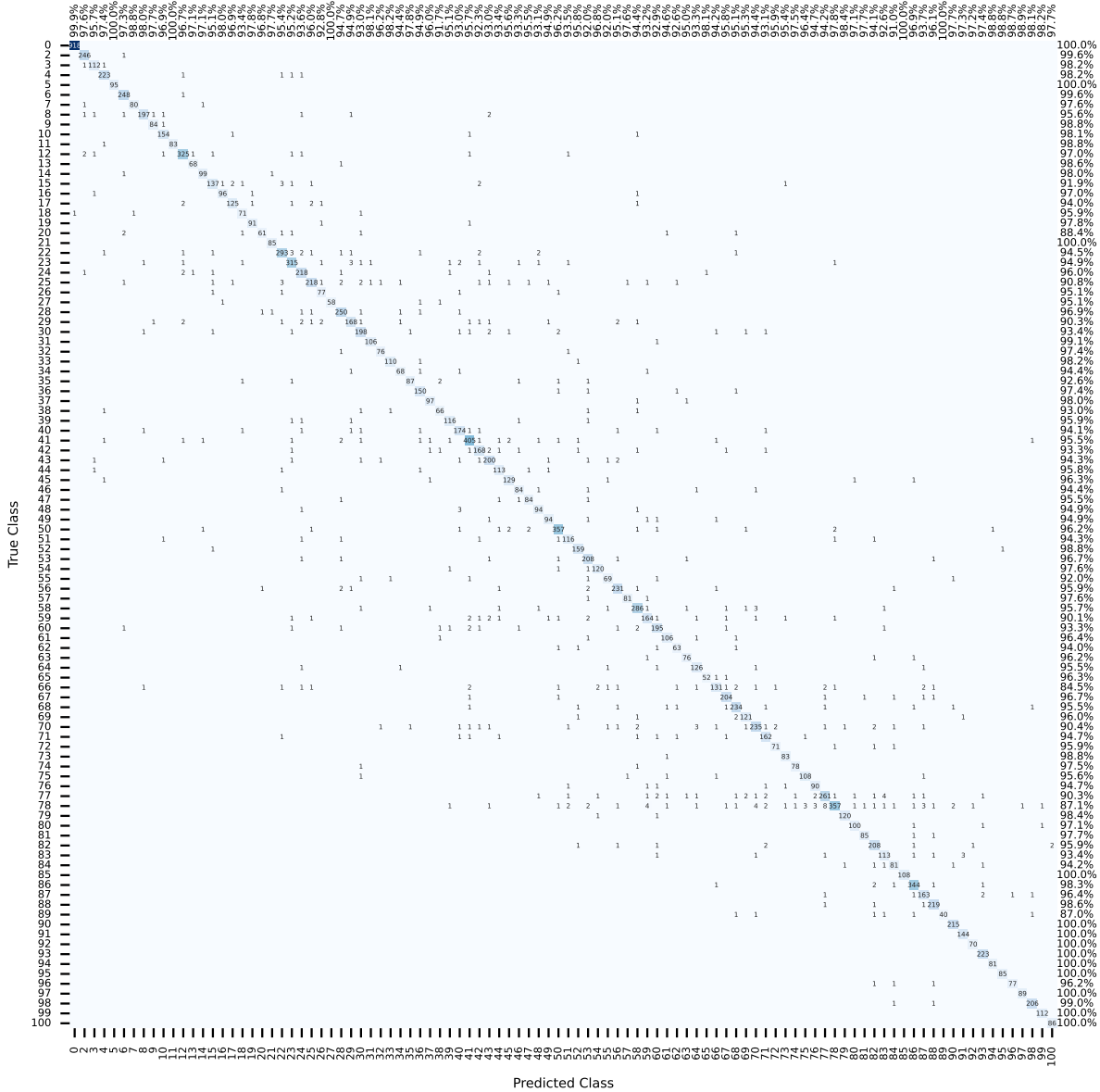


Fig. 2. Confusion matrix for the neural network-based cluster head prediction.

and $|\mathcal{D}|$ represents the cardinality of \mathcal{D} . The target output of the neural network is the set of cluster heads. The module architecture, with a depth of three, consists of three fully connected layers with 401, 2000, and 101 neurons, respectively. Each layer is followed by a ReLU activation function and a dropout layer. The output layer produces a set of probabilities using the sigmoid activation function, indicating the likelihood of each node becoming a cluster head. We divide the dataset into training and testing sets, with a ratio of 80:20. The neural network is trained using the Adam optimizer with a learning rate of $1e - 4$ and a batch size of 16. The loss function is the binary cross-entropy loss. The neural network is trained for 1000 epochs. Figure 2 presents the confusion matrix illustrating the performance of the neural network-based cluster head prediction. Row and column accuracies are

provided on the right and top sides of the confusion matrix, respectively. The neural network achieves an overall accuracy of 99.24% on the testing set. This outstanding performance is attributed to the utilization of meaningful features as input, which exhibit a high correlation with the cluster heads' feature.

The neural network architecture for the assignment of cluster members is designed to take the following parameters as input: $\alpha, \beta, \gamma, E_{net}, E_n$ for all $n \in N, E_{tx}^{sink}, E_{tx}^{(i, ch_i)}$, and CH . The vector $E_{tx}^{sink} = [E_{tx}^{ch_1}, E_{tx}^{ch_2}, \dots, E_{tx}^{ch_{|CH|}}]$ represents the energy consumption of cluster heads when transmitting data to the BS. $|CH|$ represents the cardinality of the set of cluster heads. If $|CH| < k \times |N|$, E_{tx}^{sink} is padded with zeros to match the length of CH . The vector $E_{tx}^{(i, ch_i)}$ is defined as $[E_{tx}^{(i, ch_1)}, E_{tx}^{(i, ch_2)}, \dots, E_{tx}^{(i, ch_{|CH|})}]$ for all $i \in N$ and $n \notin CH$. It represents the energy consumption

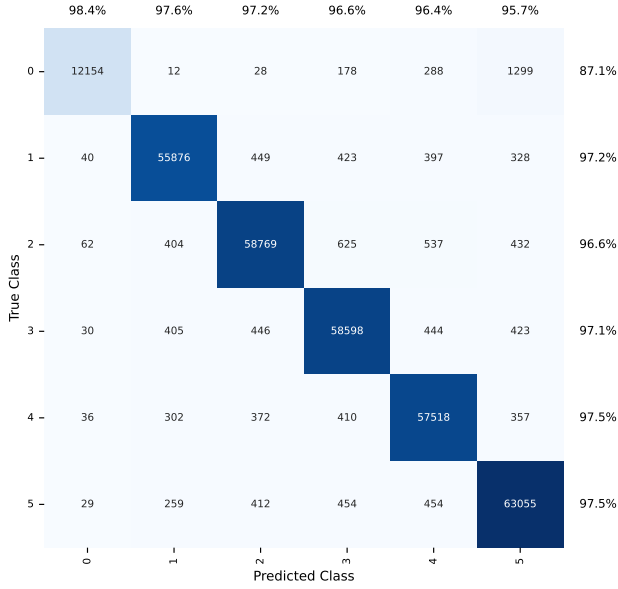


Fig. 3. Confusion matrix for the neural network-based cluster member assignment.

of cluster members when transmitting data to each cluster head. Lastly, CH is the set of cluster heads, denoted as $CH = \{CH_1, CH_2, \dots, CH_{|CH|}\}$ taken from the output of the neural network-based cluster head prediction module. The target output of the neural network is the assignment of cluster members to each $ch_i \in CH$. The module architecture, with a depth of three, consists of three fully connected layers with 703, 2000, and $|CH_{max}| \times |N|$ neurons, respectively. Where $|CH_{max}| = k \times |N|$ is the maximum number of cluster heads. The output layer is reshaped to a $(|N|, |CH_{max}|)$ matrix, where each row represents the probability distribution of a node being assigned to each $ch_i \in CH$. Each layer is followed by a ReLU activation function and a dropout layer. The output layer produces a set of probability distributions using the softmax activation function, indicating the likelihood of each node being assigned to a cluster head. The dataset is also divided into training and testing sets, with a ratio of 80:20, and the neural network is trained using the Adam optimizer with a learning rate of $1e - 6$ and a batch size of 16. The loss function is the categorical cross-entropy loss. The neural network is trained for 1000 epochs. Fig. 3 shows the confusion matrix, offering insights into the performance of the neural network-based cluster member assignment. It is noteworthy that the model predicts the cluster head index for each node based on the cluster head set. Row and column accuracies are also provided on the right and top sides of the confusion matrix, respectively. The neural network achieves an overall accuracy of 96.74% on the testing set.

C. Training RL agent and surrogate model

We use the Deep Q-Learning (DQN) algorithm to train the RL agent [29]. This algorithm is inspired by the Q-Learning algorithm, which is a model-free RL algorithm. It mainly

Algorithm 1: LEACH-RLC training and evaluation algorithm

```

Input : Network parameters,
 $\alpha, \beta, \gamma, k, E_{net}, E_n \forall n \in N, E_{tx}^{ch_j}, E_{tx}^{(i,j)},$  and  $E_{rx}^i$ 
Output: Trained RL agent/Clustering solution
Initialize replay memory  $\mathcal{D}$ , Q-network  $Q$ , and target network  $Q'$ ;
for episode  $p$  in  $\mathcal{P}$  do
  Initialize state  $s_0$ ;
  while episode  $p$  is not terminated do
    Select action  $a_t$  based on  $\epsilon$ -greedy strategy;
     $r_t \leftarrow 0$ ;
    /* Execute action  $a_t$  */
    if  $a_t = a_1$  then
      if training mode then
         $CH \leftarrow$  Predict cluster heads using the neural network;
         $CA \leftarrow$  Predict cluster member assignment using the neural network;
      end
      else
         $CH, CA \leftarrow$  Generate clustering solution using (7);
      end
       $CH_\tau \leftarrow 0$ ;
       $r_t \leftarrow r_t + 0.1$ ;
    end
    else
      Maintain the current clustering solution;
       $CH_\tau \leftarrow CH_\tau + 1$ ;
    end
     $r_t \leftarrow r_t + 1$ ;
    Observe next state  $s_{t+1}$ ;
    Store transition  $(s_t, a_t, r_t, s_{t+1})$  in  $\mathcal{D}$ ;
    Sample minibatch from  $\mathcal{D}$ ;
    Update Q-network using the sampled transitions;
    Update target network;
    if training mode then
      if  $\exists n \in N$  such that  $E_n \leq 0$  then
         $r_t \leftarrow r_t + 2$ ;
        Terminate episode  $p$ ;
      end
    end
    else
      if  $|\mathcal{D}| < 1$  then
        /* No more nodes alive */
        Terminate episode  $p$ ;
      end
    end
  end
end

```

comprises deep neural networks to approximate the action-value function, a replay memory to store the agent's experiences, and a target network to stabilize the learning process. It updates the state-action value function, also known as the Q-function, using the Bellman equation [30]. The training process of LEACH-RLC is summarized in Algorithm 1. The surrogate model to predict the clustering solution is only used during the training process. For the evaluation, we use the MILP to generate the new clusters as it provides the optimal solution. For training purposes, we set (α, β, γ) to (54.83, 14.54, 35.31), which are the optimal values obtained from the MILP formulation. We train the RL agent with the following parameters: a learning rate of $1e - 4$, a discount factor of 0.90, an exploration rate of 0.8, a batch size of 128, and a target network update frequency of 100. The agent is trained for $200k$ time steps.

TABLE III
NETWORK PARAMETERS.

Parameter	Value
N	100
L	100 m
BS location	(50, 175)
E_0	0.5 J
E_{elec}	50 nJ/bit
E_{fs}	10 pJ/bit/m ²
E_{amp}	0.0013 pJ/bit/m ⁴
F_{DA}	5 nJ/bit
B	4000 bits
B_c	1000 bits
k	0.05

VI. RESULTS

In this section, we assess the performance of LEACH-RLC by conducting a comparative analysis against LEACH and LEACH-C. The proposed clustering protocol and the RL agent are implemented using Python. The GNU Linear Programming Kit (GLPK) solver [31] is employed to solve the MILP, while the Stable Baselines3 library [32] is utilized for implementing the RL agent.

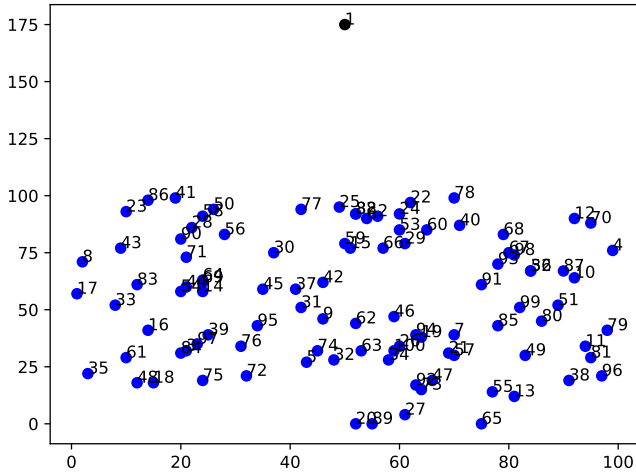


Fig. 4. Network topology.

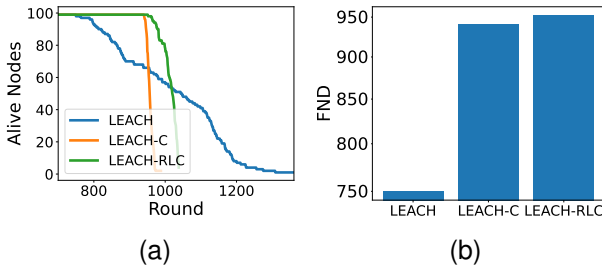


Fig. 5. Network lifetime.

The network parameters used in the simulations are outlined in Table III. Nodes are randomly deployed within a 100 m × 100 m area, with the BS strategically positioned at a considerable distance from the nodes. This setup ensures that

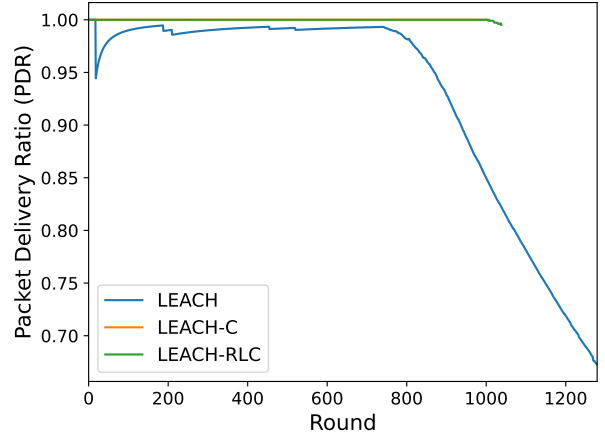


Fig. 6. Packet Delivery Ratio (PDR).

communication between the nodes and the BS occurs through the intermediary CHs, as illustrated in Fig. 4.

The performance evaluation of the protocols encompasses metrics such as network lifetime, average network energy consumption, cluster head selection, and control overhead.

Figure 5 offers a comprehensive evaluation of network lifetime, measured by the number of rounds until the occurrence of the First Node Death (FND) event. In Figure 5a, we present the behavior of alive nodes across rounds, while Figure 5b specifically illustrates the progression leading to the FND.

Highlighting results from both figures, LEACH-RLC notably outperforms its counterparts, demonstrating a remarkable network lifetime of 950 rounds compared to LEACH (750 rounds) and LEACH-C (920 rounds). Additionally, LEACH-RLC surpasses LEACH-C in the Half Node Death (HND) metric, achieving approximately 1050 rounds compared to LEACH-C’s roughly 950 rounds. This improvement can be attributed to LEACH-RLC’s ability to select Cluster Heads (CHs) and allocate nodes to clusters in a more balanced manner, as depicted in Figure 8, which illustrates the frequency of node selection as CHs.

While LEACH (Fig. 8a) tends to select scattered nodes across the network, both LEACH-C (Fig. 8b) and LEACH-RLC (Fig. 8c) prefer CHs in closer proximity to the BS. Notably, LEACH-RLC achieves a more balanced distribution of CHs for nodes with a y -coordinate greater than 50 m. This balanced distribution is credited to LEACH-RLC’s consideration of energy consumption by CHs during data transmission to the BS and data reception from their cluster members—a feature absent in LEACH-C.

Furthermore, both LEACH-RLC and LEACH-C demonstrate higher PDR than LEACH (Fig. 6) thanks to the balanced energy distribution across the network. Unlike LEACH which eventually selects nodes with low energy, causing CHs to deplete their energy within a round, resulting in a lower PDR, LEACH-RLC and LEACH-C strategically manage energy consumption, leading to improved PDR over traditional LEACH.

Additionally, LEACH-RLC’s superior performance can be linked to its lower average network energy consumption, as

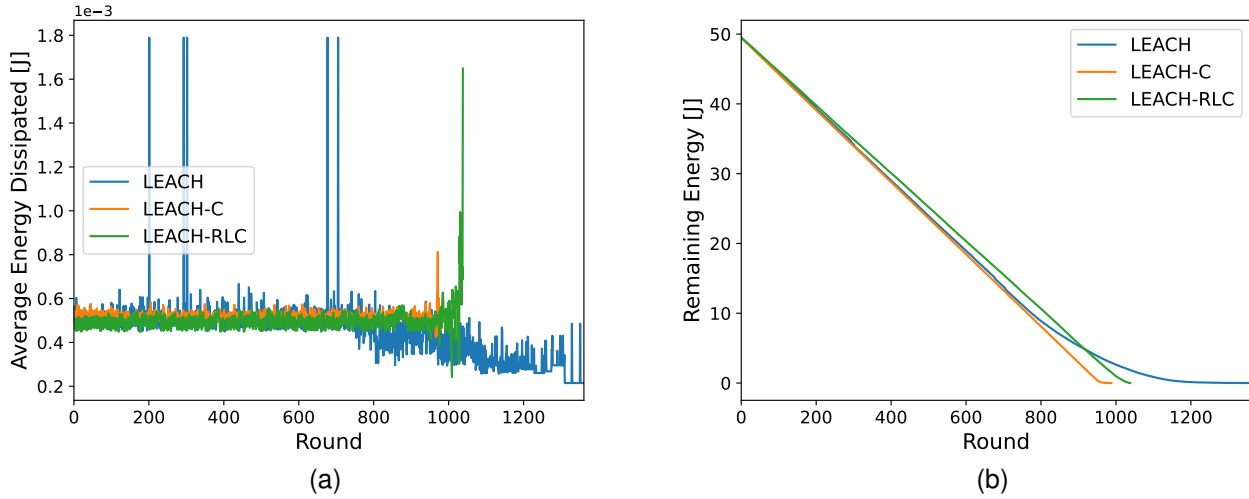


Fig. 7. Average network energy dissipated (a) and remaining energy of the network (b).

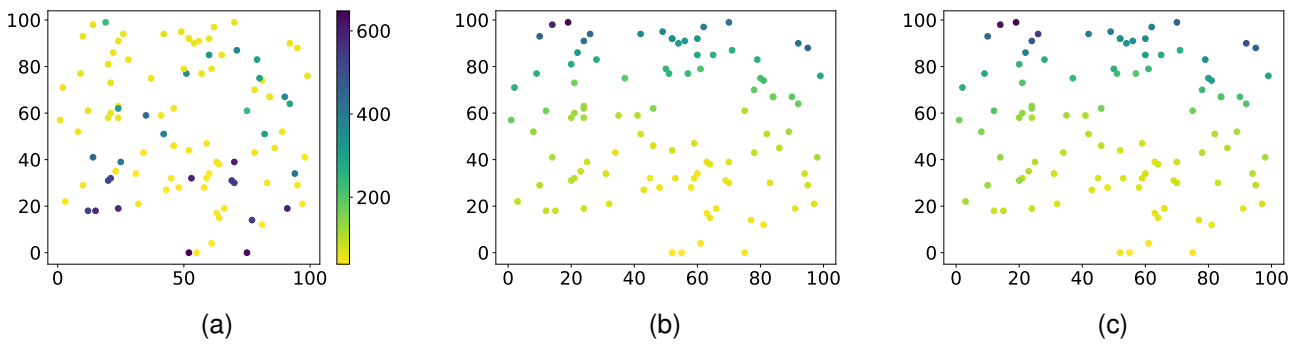


Fig. 8. Heatmap of the number of times a node is selected as a CH by each protocol. (a) shows the heatmap for LEACH, (b) shows the heatmap for LEACH-C, and (c) shows the heatmap for LEACH-RLC.

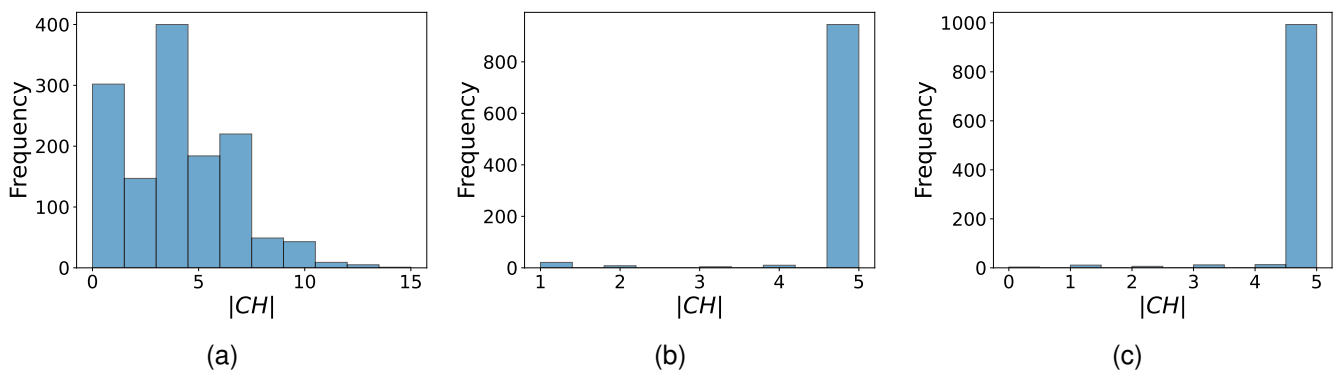


Fig. 9. Histograms of the number of CHs selected by each protocol. (a) shows the histogram for LEACH, (b) shows the histogram for LEACH-C, and (c) shows the histogram for LEACH-RLC.

evident in Fig. 7a. Notably, LEACH exhibits multiple spikes in energy consumption, indicating failed attempts to select optimal CHs due to the inherent randomness of the protocol. In this aspect, LEACH-RLC consistently outperforms both LEACH and LEACH-C. This is further corroborated in Fig. 7b, which depicts the remaining energy of the network

over rounds.

An integral aspect in achieving a balanced distribution of energy consumption across the network lies in selecting the optimal number of CHs. This key factor significantly influences the overall performance of clustering protocols. Fig. 9 visually presents the distribution of the number of

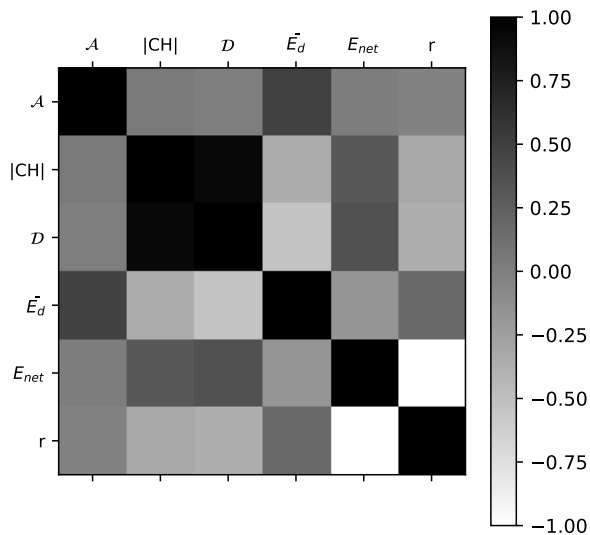


Fig. 10. Correlation matrix for the RL agent.

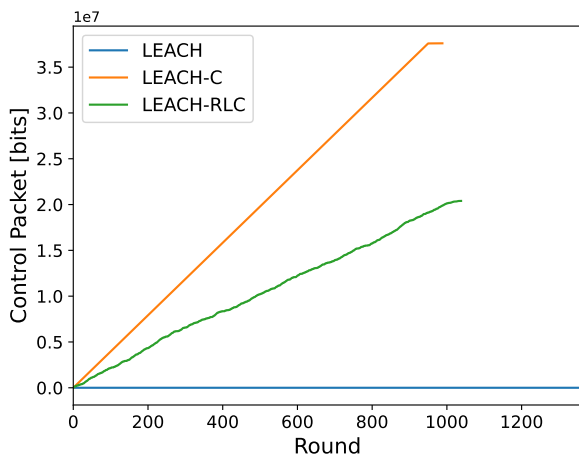


Fig. 11. Control overhead.

CHs selected by each protocol. Notably, LEACH (Fig. 9a) exhibits a wide distribution, ranging from 0 to 14 CHs. This broad spectrum is attributed to the inherent randomness of the protocol, leading to a non-uniform distribution of CHs across the network. In contrast, both LEACH-C (Fig. 9b) and LEACH-RLC (Fig. 9c) display a more uniform distribution of CHs. However, LEACH-RLC excels in achieving a superior balance in the distribution of CHs across the network. This is a noteworthy advantage, as illustrated in Fig. 8, indicating a strategic selection of CHs that contributes to the enhanced performance and energy efficiency of LEACH-RLC compared to its counterparts.

Now, delving deeper into the performance analysis of LEACH-RLC, we examine the correlation between network parameters and the number of selected CHs by the RL agent.

Fig. 10 illustrates the correlation matrix for the RL agent. Notably, the action taken by the RL agent exhibits a high correlation with the average energy dissipated by the nodes (\bar{E}_d), suggesting that the agent triggers a new action in response to changes in average energy dissipation.

This observation is corroborated in Fig. 12, where we depict the average network energy consumption vs. the actions taken by the RL agent (keeping the same set of CHs or generating new CHs). Notably, LEACH (Fig. 12a) generates more new CHs than LEACH-C (Fig. 12b) and LEACH-RLC (Fig. 12c) due to its decentralized nature, neglecting the overall energy consumption of the network. Conversely, LEACH-C and LEACH-RLC consider the network’s overall energy consumption, with LEACH-RLC showing a more uniform distribution of new CHs for higher values of average network energy consumption.

Fig. 13 further highlights the frequency of generating new CHs over rounds. LEACH-RLC (Fig. 13c) exhibits a less frequent generation of new CHs compared to LEACH (Fig. 13a) and LEACH-C (Fig. 13b), reflecting the agent’s adaptive evaluation of the network state at each round. The agent weighs the performance of maintaining the current set of CHs against generating new CHs, effectively reducing control overhead, as evidenced in Fig. 11. LEACH-RLC consistently presents lower control overhead than LEACH-C, demonstrating the efficacy of the RL agent in learning the optimal timing for control message transmission, a capability absent in LEACH-C. Although LEACH exhibits zero control overhead, it does not guarantee an even distribution of CHs across the network, as demonstrated in previous figures.

A. Research Questions Analysis

The evaluation of LEACH-RLC provides meaningful insights into the posed research questions. Firstly, regarding *RQ1*, our results showcase that LEACH-RLC successfully reduces control overhead while maintaining or even enhancing network performance. The intelligent clustering strategy, coupled with the adaptive RL agent, ensures that the network operates efficiently without unnecessary overhead.

Moving on to *RQ2*, the optimal frequency for generating new clustering solutions is a critical aspect of network management. Our findings reveal that LEACH-RLC dynamically adjusts the generation of new clusters based on the energy dynamics and network conditions. This adaptability ensures an optimal balance, contributing to the extended network lifetime observed in our experiments.

Finally, addressing *RQ3*, the opportune moment for triggering a new clustering solution is intricately linked to the energy consumption patterns. LEACH-RLC demonstrates a keen understanding of the network state, generating new clusters judiciously when energy consumption increases. This strategic decision-making process significantly contributes to maintaining a balanced distribution of energy and prolonging the network’s operational lifespan.

VII. CONCLUSION

In this paper, we introduced LEACH-RLC, an innovative clustering protocol designed to enhance the performance of

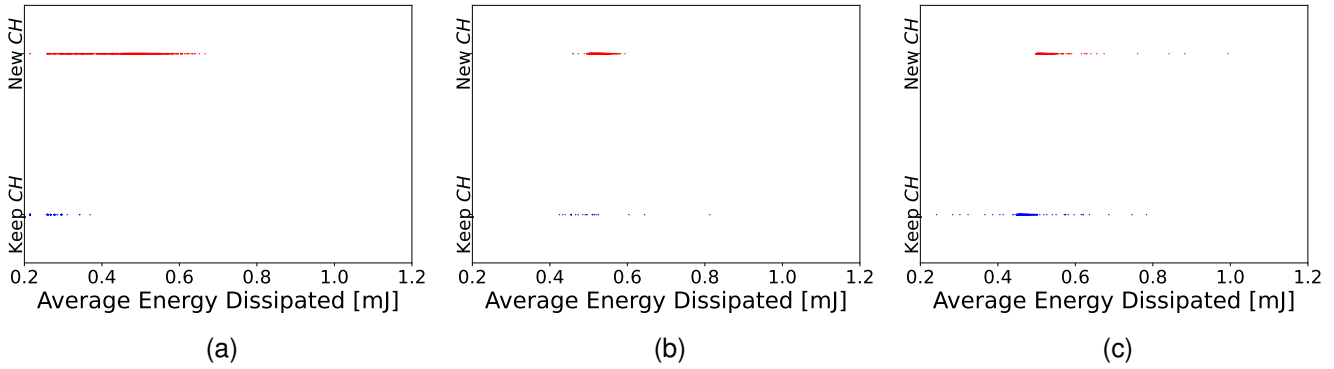


Fig. 12. Average network energy consumption vs. frequency of new CHs. (a) shows the results for LEACH, (b) shows the results for LEACH-C, and (c) shows the results for LEACH-RLC.

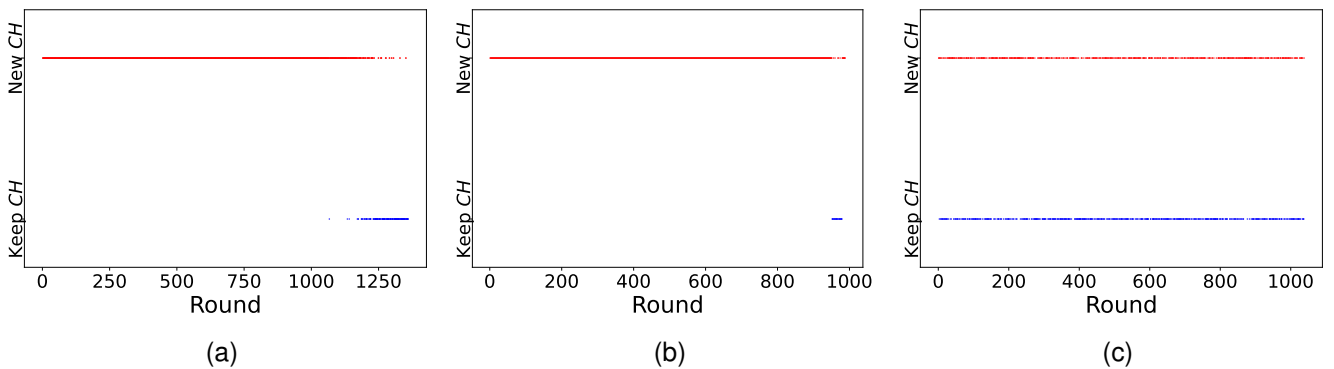


Fig. 13. Frequency of new CHs over rounds. (a) shows the results for LEACH, (b) shows the results for LEACH-C, and (c) shows the results for LEACH-RLC.

WSN applications. Leveraging a MILP, LEACH-RLC intelligently selects CHs and efficiently assigns nodes to clusters. A key feature of LEACH-RLC is its incorporation of a RL agent, which significantly reduces control overhead by learning the optimal timing for generating new clusters.

The RL agent in LEACH-RLC employs a surrogate model, effectively estimating cluster heads and cluster members to expedite the learning process. Our comprehensive evaluation of LEACH-RLC delves into various performance metrics, including network lifetime, average energy consumption, control overhead, number of cluster heads, and the frequency of new cluster generation.

Results from the evaluation provide valuable insights into the optimal configuration of LEACH-RLC, shedding light on the parameters that significantly influence its performance. Particularly, the protocol’s ability to balance energy consumption among nodes leads to a prolonged network lifetime. This superior performance is attributed to LEACH-RLC’s refined selection of CHs and their assignment to clusters.

Furthermore, our exploration into the correlation between network parameters and RL agent actions unveils the agent’s adaptability to changing energy dynamics. The RL agent demonstrates a nuanced response to the average energy dissipation of nodes, showcasing a balanced distribution of new CHs generation for varying levels of energy consumption.

The answers to our research questions affirm that LEACH-RLC effectively reduces control overhead without compromis-

ing network performance, determines the optimal frequency for generating new clusters, and strategically triggers new clustering solutions based on the network’s energy dynamics. These findings underscore the protocol’s adaptability and efficiency in achieving prolonged network lifespan and energy balance.

This study not only advances the understanding of LEACH-RLC but also contributes valuable insights to the broader field of WSNs. Future research could explore additional dimensions of LEACH-RLC optimization, further refining its parameters and expanding its applicability across diverse WSN scenarios.

REFERENCES

- [1] L. Atzori, A. Iera, and G. Morabito, “The internet of things: A survey,” *Computer networks*, vol. 54, no. 15, pp. 2787–2805, 2010.
- [2] K. Schwab, *The fourth industrial revolution*. Currency, 2017.
- [3] T. Qiu, N. Chen, K. Li, M. Atiquzzaman, and W. Zhao, “How can heterogeneous internet of things build our future: A survey,” *IEEE Commun. Surveys Tuts.*, vol. 20, no. 3, pp. 2011–2027, 2018.
- [4] M. S. Batta, H. Mabeed, Z. Aliouat, and S. Harous, “Battery state-of-health prediction-based clustering for lifetime optimization in iot networks,” *IEEE Internet Things J.*, vol. 10, no. 1, pp. 81–91, 2022.
- [5] J. Luo, Y. Chen, M. Wu, and Y. Yang, “A survey of routing protocols for underwater wireless sensor networks,” *IEEE Commun. Surveys Tuts.*, vol. 23, no. 1, pp. 137–160, 2021.
- [6] Z. Cai, Q. Chen, T. Shi, T. Zhu, K. Chen, and Y. Li, “Battery-free wireless sensor networks: A comprehensive survey,” *IEEE Internet Things J.*, 2022.
- [7] W. R. Heinzelman, A. Chandrakasan, and H. Balakrishnan, “Energy-efficient communication protocol for wireless microsensor networks,” in *Proc. 33rd HICSS*. IEEE, 2000, pp. 10–pp.

- [8] W. B. Heinzelman, A. P. Chandrakasan, and H. Balakrishnan, "An application-specific protocol architecture for wireless microsensor networks," *IEEE Trans. Wireless Commun.*, vol. 1, no. 4, pp. 660–670, 2002.
- [9] T. M. Behera, S. K. Mohapatra, U. C. Samal, M. S. Khan, M. Daneshmand, and A. H. Gandomi, "Residual energy-based cluster-head selection in wsn for iot application," *IEEE Internet Things J.*, vol. 6, no. 3, pp. 5132–5139, 2019.
- [10] Y. Fathy and P. Barnaghi, "Quality-based and energy-efficient data communication for the internet of things networks," *IEEE Internet Things J.*, vol. 6, no. 6, pp. 10318–10331, 2019.
- [11] P. Chithaluru, S. Kumar, A. Singh, A. Benslimane, and S. K. Jangir, "An energy-efficient routing scheduling based on fuzzy ranking scheme for internet of things," *IEEE Internet Things J.*, vol. 9, no. 10, pp. 7251–7260, 2021.
- [12] T. M. Behera, S. K. Mohapatra, U. C. Samal, M. S. Khan, M. Daneshmand, and A. H. Gandomi, "I-sep: An improved routing protocol for heterogeneous wsn for iot-based environmental monitoring," *IEEE Internet Things J.*, vol. 7, no. 1, pp. 710–717, 2019.
- [13] C. Chen, L.-C. Wang, and C.-M. Yu, "D2crp: A novel distributed 2-hop cluster routing protocol for wireless sensor networks," *IEEE Internet Things J.*, vol. 9, no. 20, pp. 19575–19588, 2022.
- [14] J.-S. Lee and H.-T. Jiang, "An extended hierarchical clustering approach to energy-harvesting mobile wireless sensor networks," *IEEE Internet Things J.*, vol. 8, no. 9, pp. 7105–7114, 2020.
- [15] J.-S. Lee and C.-L. Teng, "An enhanced hierarchical clustering approach for mobile sensor networks using fuzzy inference systems," *IEEE Internet Things J.*, vol. 4, no. 4, pp. 1095–1103, 2017.
- [16] M. Ahmad, T. Li, Z. Khan, F. Khurshid, and M. Ahmad, "A novel connectivity-based leach-meec routing protocol for mobile wireless sensor network," *Sensors*, vol. 18, no. 12, p. 4278, 2018.
- [17] S. Mohapatra, P. K. Behera, P. K. Sahoo, S. K. Bisoy, K. L. Hui, and M. Sain, "Mobility induced multi-hop leach protocol in heterogeneous mobile network," *IEEE Access*, vol. 10, pp. 132 895–132 907, 2022.
- [18] J. Zhang and R. Yan, "Centralized energy-efficient clustering routing protocol for mobile nodes in wireless sensor networks," *IEEE Commun. Lett.*, vol. 23, no. 7, pp. 1215–1218, 2019.
- [19] X. Chen, G. Sun, T. Wu, L. Liu, H. Yu, and M. Guizani, "Rance: A randomly centralized and on-demand clustering protocol for mobile ad hoc networks," *IEEE Internet Things J.*, vol. 9, no. 23, pp. 23 639–23 658, 2022.
- [20] K. Tebessi and F. Semchedine, "An improvement on leach-c protocol (leach-cmsn)," *Autom. Control. Comput. Sci.*, vol. 56, no. 1, pp. 10–16, 2022.
- [21] M. Gamal, N. E. Mekky, H. Soliman, and N. A. Hikal, "Enhancing the lifetime of wireless sensor networks using fuzzy logic leach technique-based particle swarm optimization," *IEEE Access*, vol. 10, pp. 36 935–36 948, 2022.
- [22] R. Jin, X. Fan, and T. Sun, "Centralized multi-hop routing based on multi-start minimum spanning forest algorithm in the wireless sensor networks," *Sensors*, vol. 21, no. 5, p. 1775, 2021.
- [23] N. Ma, H. Zhang, H. Hu, and Y. Qin, "Escvad: an energy-saving routing protocol based on voronoi adaptive clustering for wireless sensor networks," *IEEE Internet Things J.*, vol. 9, no. 11, pp. 9071–9085, 2021.
- [24] C. Szepesvári, *Algorithms for reinforcement learning*. Springer Nature, 2022.
- [25] N. C. Luong, D. T. Hoang, S. Gong, D. Niyato, P. Wang, Y.-C. Liang, and D. I. Kim, "Applications of deep reinforcement learning in communications and networking: A survey," *IEEE Commun. Surveys Tuts.*, vol. 21, no. 4, pp. 3133–3174, 2019.
- [26] F. F. Jurado-Lasso, L. Marchegiani, J. F. Jurado, A. M. Abu-Mahfouz, and X. Fafoutis, "A survey on machine learning software-defined wireless sensor networks (ml-sdwsns): Current status and major challenges," *IEEE Access*, vol. 10, pp. 23 560–23 592, 2022.
- [27] F. F. Jurado-Lasso, C. Orfanidis, J. Jurado, and X. Fafoutis, "Hrl-tsch: A hierarchical reinforcement learning-based tsch scheduler for iiot," 2024, preprint on arXiv: <https://doi.org/10.48550/arXiv.2401.10368>.
- [28] F. F. Jurado-Lasso, M. Barzegaran, J. F. Jurado, and X. Fafoutis, "Elise: A reinforcement learning framework to optimize the slotframe size of the tsch protocol in iot networks," 2023, preprint on TechRxiv: <https://doi.org/10.36227/techrxiv.23212442.v3>.
- [29] T. Hester, M. Vecerik, O. Pietquin, M. Lanctot, T. Schaul, B. Piot, D. Horgan, J. Quan, A. Sendonaris, I. Osband *et al.*, "Deep q-learning from demonstrations," in *Proc. 32nd AAAI*, vol. 32, no. 1, 2018.
- [30] C. J. Watkins and P. Dayan, "Q-learning," *Machine learning*, vol. 8, pp. 279–292, 1992.
- [31] A. Makhorin, "Glpk (gnu linear programming kit)," 2008, <https://www.gnu.org/software/glpk/>.
- [32] A. Raffin, A. Hill, A. Gleave, A. Kanervisto, M. Ernestus, and N. Dornmann, "Stable-baselines3: Reliable reinforcement learning implementations," *JMLR*, vol. 22, no. 1, pp. 12 348–12 355, 2021.

F. Fernando Jurado-Lasso (GS'18-M'21) received the Ph.D. degree in Engineering and the M.Eng. degree in Telecommunications Engineering both from The University of Melbourne, Melbourne, VIC, Australia, in 2020 and 2015, respectively; a B.Eng. degree in Electronics Engineering in 2012 from the Universidad del Valle, Cali, Colombia. He is currently a postdoctoral researcher at the Embedded Systems Engineering (ESE) section of the Department of Applied Mathematics and Computer Science of the Technical University of Denmark (DTU Compute).

His research interests include networked embedded systems, software-defined wireless sensor networks, machine learning, protocols and applications for the Internet of Things.

J. F. Jurado received the Doctorate and MSc degree in Physics both from Universidad del Valle, Cali, Colombia, in 2000 and 1986, respectively; he also holds a BSc degree in Physics from the Universidad de Nariño, Pasto, Colombia in 1984. He is currently a Professor with the Faculty of Engineering and Administration of the Department of Basic Science of The Universidad Nacional de Colombia Sede Palmira, Colombia. His research interests include nanomaterials, magnetic and ionic materials, nanoelectronics, embedded systems and the Internet of Things. He is a senior member of Minciencias in Colombia.

Xenofon Fafoutis (S'09-M'14-SM'20) received a PhD degree in Embedded Systems Engineering from the Technical University of Denmark in 2014; an MSc degree in Computer Science from the University of Crete (Greece) in 2010; and a BSc in Informatics and Telecommunications from the University of Athens (Greece) in 2007. He is currently an Associate Professor with the Embedded Systems Engineering (ESE) section of the Department of Applied Mathematics and Computer Science of the Technical University of Denmark (DTU Compute). His research interests primarily lie in Wireless Embedded Systems as an enabling technology for Digital Health, Smart Cities, and the (Industrial) Internet of Things (IIoT).